Arginine butyrate: a therapeutic candidate for Duchenne muscular dystrophy.

Sara Vianello, Hua Yu, Vincent Voisin, Hafedh Haddad, Xun He, Arthur S. Foutz, Catherine Sebrié, Brigitte Gillet, Morgane Roulot, Françoise Fougerousse, et al.

Arginine butyrate: a therapeutic candidate for Duchenne muscular dystrophy

Sara Vianello,[*,1] Hua Yu,[*,1] Vincent Voisin,[*] Hafedh Haddad,[*] Xun He,[*] Arthur S. Foutz,[†] Catherine Sebrié,[‡,2] Brigitte Gillet,[‡,2] Morgane Roulot,[*] Françoise Fougerousse,[§] Caroline Perronnet,[‖,¶,3] Cyrille Vaillend,[‖,¶] Stefan Matecki,[#] Diana Escolar,[**] Laura Bossi,[††] Maurice Israël,[*] and Sabine de la Porte[*,4]

[*]Neurobiologie & Développement–Unité Propres de Recherche (UPR) 3294 and [†]Neurobiologie Génétique et Intégrative–UPR 2216, Centre National de la Recherche Scientifique (CNRS), Institut de Neurobiologie Alfred Fessard–FRC2118, Gif sur Yvette, France; [‡]CNRS, Institut de Chimie des Substances Naturelles, Résonance Magnétique Nucléaire(RMN) Biologique, Gif sur Yvette, France; [§]Généthon, Evry, France; [‖]Université Paris-Sud, Centre de Neurosciences Paris-Sud, and [¶]CNRS, Unité Mixte de Recherche (UMR) 8195, Orsay, France; [#]Institut National de la Santé et de la Recherche Médicale (INSERM), Equipe Région INSERM (ERI), Muscle et Pathologies, Centre Hospitalier Universitaire (CHU) A. de Villeneuve, Université de Montpellier, Montpellier, France; [**]Johns Hopkins School of Medicine, Baltimore, Maryland, USA; and [††]Domain Therapeutics, BioParc, Illkirch, France

ABSTRACT **As a strategy to treat Duchenne muscular dystrophy, we used arginine butyrate, which combines two pharmacological activities: nitric oxide pathway activation, and histone deacetylase inhibition. Continuous intraperitoneal administration to dystrophin-deficient *mdx* mice resulted in a near 2-fold increase in utrophin (protein homologous to dystrophin) in skeletal muscle, heart, and brain, accompanied by an improvement of the dystrophic phenotype in both adult and newborn mice (45 and 70% decrease in creatine kinase level, respectively; 14% increase in tidal volume, 30% decrease in necrotic area in limb and 23% increase in isometric force). Intermittent administration, as performed in clinical trials, was then used to reduce the frequency of injections and to improve safety. This also enhanced utrophin level around 2-fold (EC_{50}=284 mg/ml) and alleviated the dystrophic phenotype (inverted grid and grip test performance near to wild-type values, creatine kinase level decreased by 50%). Skin biopsies were used to monitor treatment efficacy, instead of invasive muscle biopsies, and this could be done a few days after the start of treatment. A 2-fold increase in utrophin expression was also shown in cultured human myotubes. *In vivo* and *in vitro* experiments demonstrated that the drug combination acts synergistically. Together, these data constitute a proof of principle of the beneficial effects of arginine butyrate on muscular dystrophy.—Vianello, S., Yu, H., Voisin, V., Haddad, H., He, X., Foutz, A. S., Sebrié, C., Gillet, B., Roulot, M., Fougerousse, F., Perronnet, C., Vaillend, C., Matecki, S., Escolar, D., Bossi, L., Israël, M., de la Porte, S. Arginine butyrate: a therapeutic candidate for Duchenne muscular dystrophy. *FASEB J.* 27, 2256–2269 (2013). www.fasebj.org**

Key Words: DMD · mdx · pharmacology · treatment · NO · histone deacetylase

Duchenne muscular dystrophy (DMD), a lethal X-linked recessive disorder, is characterized by progressive muscle degeneration due to the lack of expression of dystrophin, a cytoskeletal protein essential to muscle structure and function. Loss of muscle strength is typically observed at the age of 4–5 yr, and the disease leads to death due to cardiac or respiratory failure by the age of 25–30. Although various curative therapeutic approaches, such as cell, gene, and pharmacological therapies, are currently being investigated, they still show some limitations (1) and at present, only corticosteroids have a palliative effect on the disease, albeit with severe side effects. Thus, new approaches to com-

Abbreviations: 3D, 3-dimensional; AB, arginine butyrate; AB_{cf}, arginine butyrate clinical formulation; CK, creatine kinase; DAG, dystrophin-associated glycoprotein; DAP, dystrophin-associated protein; DMD, Duchenne muscular dystrophy; f_R, respiratory frequency; MRI, magnetic resonance imaging; NO, nitric oxide; qPCR, quantitative polymerase chain reaction; TA, tibialis anterior; V_E, minute ventilation; V_T, tidal volume; WT, wild type

[1] These authors contributed equally to this work.

[2] Current address: CNRS, U2R2M-UMR8081, Orsay, F-91405, France.

[3] Current address: Department of Cellular and Physiological Sciences, University of British Columbia, Vancouver, BC, Canada.

[4] Correspondence: CNRS, Ave. de la Terrasse, Bat. 32/33, Institut de Neurobiologie Alfred Fessard, Neurobiologie & Développement-UPR 3294 CNRS, Gif sur Yvette, F-91198, France. E-mail: sabine.delaporte@inaf.cnrs-gif.fr

pensate for the lack of dystrophin are warranted. Whatever the pharmacological strategy envisaged to reverse the dystrophic phenotype in patients with DMD, it cannot be effective without restoration of dystrophin expression or overexpression of utrophin, to compensate for the absence of dystrophin. A treatment must restore sarcolemmal integrity (2).

Utrophin is a cytoskeletal protein that shares >80% sequence homology with dystrophin and has similar cellular functions (3). Under some conditions, the utrophin gene is naturally induced to resume function, as seen in DMD (4), in which the gene is up-regulated and low-level utrophin expression expands to the entire cytoskeletal membrane, in an inadequate attempt to compensate for the lack of dystrophin. Further reactivation and renewed expression of utrophin can be exogenously induced by gene (5, 6) or pharmacological therapies (2). A 2-fold up-regulation of utrophin is sufficient to alleviate dystrophic muscle pathology (7). The main advantage of up-regulating utrophin by pharmacological therapies is that there is no need for dystrophin gene replacement or repair. Moreover, targeting the muscles of the whole body appears to be easy with standard modes of administration.

One way to up-regulate utrophin expression is through stimulation of the nitric oxide (NO) pathway. Our previous studies showed that an effective activator of the NO pathway, L-arginine, increases utrophin levels in muscles and targets utrophin to the sarcolemma *in vivo* and *in vitro* (8, 9). In normal and *mdx* myotubes in culture, L-arginine and NO increase utrophin levels and enhance its membrane localization. The NO-induced increase in utrophin expression does not occur with D-arginine, L-NAME (an inhibitor of NO synthase), or oxadiazolo-quinoxalin-1-one (ODQ; an inhibitor of a soluble guanylate cyclase involved in the effects of NO), thus showing the involvement of NO synthase in this process (8). Improvement of dystrophic phenotypes *via* the NO pathway has been demonstrated by many studies in dystrophin-deficient *mdx* mice. Isometric force and resistance to eccentric contractions can thus be improved, serum creatine kinase (CK) levels reduced, muscle structure restored, muscle regeneration increased (10–18), inflammation reduced [decreases in nuclear factor (NF)-κB level and activity; ref, 19], and finally, a normal phosphatidylcholine ion peak intensity ratio of the muscular membrane can be restored (20). NO inducers may have other beneficial effects. First, NO may induce the vasodilatation required for effective supply of metabolites and oxygen to the working muscle, probably by counterbalancing the vasoconstrictor effect of the sympathetic adrenergic system (21, 22). Secondly, the expression of utrophin in vessels, *via* the NO produced by endothelial NOS, could compensate for the lost dystrophin.

Interestingly, the group of Perrine and Faller (23) has shown that administration of butyrate to treat β-globin disorders (sickle-cell disease and β-thalassemia) renewed expression of a fetal form of hemoglobin in erythroid progenitors of patients. Butyrate's effect is hypothesized to occur *via* the inhibition of histone deacetylases, leading to hyperacetylation of histone cores and activation of previously silenced genes. More recent clinical trials to treat β-globin disorders have used arginine butyrate (AB) in place of sodium butyrate to avoid toxicity due to sodium excess, and have demonstrated its safety for pediatric patients (24). Data from safety pharmacology studies (single-dose studies, repeated-dose toxicology, genotoxicity/mutagenicity, pharmacokinetics, and products of metabolism) demonstrate a favorable benefit/risk ratio, suggesting that AB could be used in patients with DMD. These data prompted us to evaluate whether the capacity of AB to renew fetal gene expression could be exploited in treatment of DMD, as utrophin can be considered as a fetal homologue of dystrophin. This hypothesis was further supported by recent studies showing alleviation of the dystrophic phenotype in *mdx* mice after treatment with trichostatin (25) and valproic acid (26), two distinct histone deacetylase inhibitors.

In the present study, our main goal was the preclinical evaluation of the effects of AB on the myopathy displayed in the *mdx* mouse model of DMD. As described above, we consider that AB combines two pharmacological activities that have been shown to be beneficial to the dystrophic phenotype, *i.e.*, NO pathway activation by arginine, and histone deacetylase inhibition by butyrate. Previous work initiated in the framework of a partnership with the pharmaceutical company Domain Therapeutics was performed using a high dose of AB (250 instead of 100 mg/kg/d, the optimal dose selected in chronic administration in the current study) for a long period (6 mo). This resulted in only modest beneficial effects in *mdx* mice, yet safety was good compared with prednisone (1 mg/kg/d), a corticosteroid with toxic effects (27). In the first part of the present study, we used the chronic protocol with lower doses of AB and a range of technical approaches with the aim of providing a proof of principle that AB can increase utrophin expression in muscle tissues and alleviate the dystrophic phenotype in *mdx* mice. The possible synergistic action of arginine and butyrate was addressed by assaying serum CK as a biomarker of muscle necrosis. We further detailed the phenotypic impact of this treatment at various levels, including utrophin and dystroglycan expression in distinct muscle types, effects of administration in newborn *vs.* adult mice, impact on muscle degeneration, respiratory function, body and muscle weights, and on isometric muscle force. Continuous perfusions cannot be easily considered in such a population, hence the importance of evaluating the effectiveness of intermittent administration. Toxicity studies indicate that in rat and dog, toxic effects are localized at the injection site (catheter) and are considered to be sequelae of the inflammation associated with continuous i.v. infusion (28). Because intermittent injections seem more appropriate for potential application to the human condition, the second part of our study was based on a protocol of intermittent injections that mimics protocols previously used to

treat thalassemic children (24). Future clinical trials will address ambulatory patients with DMD (9–11 yr old) with a comparable administration procedure. The goal was then to determine if this specific protocol would recapitulate the basic effects of AB: increased utrophin and dystroglycan expression, body weight increase, reduced CK levels and increased muscle strength, which constitute a restricted but relevant set of biomarkers of reduced myopathy. We also used very short injection schedules and specific biochemical markers to assess the possibility of a rapid evaluation of treatment effects in both animal and human biopsy material. Application to the human condition is supported by the observation of utrophin protein upregulation in human myotubes treated with AB. The comparison of chromatin acetylation states in human myotubes treated with L-arginine, butyrate, and AB confirmed that the combined formula of AB acts synergistically.

MATERIALS AND METHODS

AB preparation

L-arginine was prepared in MilliQ water (Millipore, Billerica, MA, USA) and *n*-butyric acid (Sigma-Aldrich, Lyon, France) was added to make 2 distinct stock solutions: a 26% solution (1 M arginine/1 M butyrate, pH 7) was used for continuous-chronic injections, as described previously (29), whereas a 12.5% solution (0.76 M arginine/1 M butyrate, pH 5.5) was used for intermittent injections (see below). The latter was adapted from U.S. Food and Drug Administration recommendations (personal communication) and corresponds exactly to the AB clinical formulation (AB_{cf}) currently used for administration to patients with β hemoglobinopathies. The stock solutions were diluted before use in 0.9% NaCl to obtain both injectable AB solutions.

Mouse experimental procedures

Since DMD is an X-linked genetic disorder, studies were performed using male mice. All experiments were performed in accordance with the guidelines established by the European Communities Council Directive (Guide for the Care and Use of Laboratory Animals: EEC86/609 Council Directive-Decree 2001-131).

Adult *mdx* and wild-type (WT) mice of the C57BL/10 strain were aged 8 wk at the start of experiments. The newborn mice were injected from postnatal d 2 or 3. Treatment was administered by intraperitoneal injection (1 ml/100 g body weight). Two main protocols of administration were used: continuous-chronic and intermittent. In the continuous-chronic treatment protocol, the mice received 1 daily injection, 5 d/wk for 6 wk. Adult animals were assigned to the saline group injected with 0.9% NaCl or to the treated group injected with either AB at 5, 25, 50, 100, 200, and 300 mg/kg/d or with butyrate alone (Sigma-Aldrich) at 5, 45, 50, 55, 60, and 80 mg/kg/d or L-arginine (Sigma-Aldrich) alone at 100, 200, 500, 800, and 1000 mg/kg/d. For the treatment of newborn mice, preliminary experiments were necessary to adjust the doses, which were 5, 10, 25, 50, 60, and 80 mg/kg/d. In the intermittent treatment protocol, adult mice were injected with saline (0.9% NaCl) or AB_{cf} doses (100, 200, 500, 600, 800, and 1000 mg/kg/d) as a series of 4 consecutive daily injections every 2 or 3 wk for 6 wk. One single series of 4 consecutive daily injections was also used to assess the early effects of this treatment, and the mice were then euthanized the day after (d 5) or 1 wk later (d 12).

Animals were weighed before each injection. *In vivo* functional evaluations were performed in a blinded fashion and carried out 24 h after the end of the treatment. Then, the mice were anesthetized with 10% pentobarbital sodium, blood samples were taken from the heart for measurement of serum CK levels, and mice were sacrificed by cervical dislocation; the muscles and brain were dissected out and frozen for molecular and biochemical analyses.

Immunofluorescence

After fixation in cold methanol (+4°C for 10 min), cryostat sections (7 μm) of muscles or culture dishes of human myotubes were incubated for 5 h at room temperature with a polyclonal antiutrophin antibody (mouse tissue: C19, 1:150 dilution; human tissue: N19, 1:100 dilution; Santa Cruz Biotechnology, Santa Cruz, CA, USA) and/or with a monoclonal anti-β-dystroglycan antibody (NCL-β-DG, 1:10 dilution: Novocastra, Newcastle-on-Tyne, UK), and/or with a monoclonal anti-embryonic myosin antibody (NCL-MHCd, 1:100 dilution; Novocastra) then for 1 h with fluorescent secondary antibody (polyclonal anti-goat Cy2 antibody diluted 1:1000 and monoclonal anti-mouse Cy3 antibody diluted 1:5000; Jackson Immunoresearch, Bar Harbor, ME, USA). Tissue sections were observed using a Leica DM RXA2 fluorescent-imaging microscope (Leica Microsystems, Wetzlar, Germany). Image capture was performed with a CoolSNAP camera (Roper Scientific, Trenton, NJ, USA) and Openlab software (Improvision, Coventry, UK).

Immunoblot analyses

The proteins were extracted from muscle, brain, and skin samples, as well as from cultured myotubes, in a buffer containing 10 mM Tris-HCl, 1 mM EDTA, and 10% SDS (pH 6.8). The total protein content was determined according to DC Protein Assay protocol (Bio-Rad, Hercules, CA, USA). Proteins were separated by SDS-PAGE on a 6–12% multiplex gel (12% for the histone H3 acetylation antibody; X-Cell II Mini Cell; Invitrogen, Saint Aubin, France) with a molecular weight marker (Rainbow; Amersham Pharmacia Biotech, Piscataway, NJ, USA) and then electroblotted onto an Immobilon-P polyvinyl membrane. We applied Coomassie G250 stain to verify the equal loading of gels.

The membrane was incubated with monoclonal antibodies against utrophin (NCL-DRP 2, 1:250 dilution; Novocastra), β-dystroglycan (NCL-β-DG, 1:50 dilution; Novocastra) embryonic myosin (anti-embryonic myosin (2B6), 1:50 dilution, a gift from Gillian Butler-Browne, Institut de Myologie, Paris, France) and/or the acetylated part of histone H3 (Lys 9; AcH3K9, 1:1000 dilution; Upstate-Millipore), and then with a secondary sheep anti-mouse antibody linked to horseradish peroxidase (1:4000 dilution; Jackson Immunoresearch). Immunostaining was revealed by a chemiluminescent reaction (ECL; Amersham Pharmacia Biotech). Desmin (53 kDa) and actin (43 kDa) were used as loading controls for muscle and brain extracts, respectively (desmin is not expressed in brain). Band intensity was quantified using Claravision analyzer software (Claravision, Paris, France). Experiments were repeated ≥3 times. For each experiment, the results in treated mice were normalized to the values obtained in saline-injected mice (treated/saline ratio). Quantification was performed on films obtained after different exposure times for distinct proteins (~30 s for β-dystroglycan, 2 min for desmin and

utrophin), but within quantifications of a given target protein, the same exposure times were used for the different doses shown on the histograms.

Quantitative polymerase chain reaction (qPCR) analysis

RNA was extracted using a standard protocol with TRIzol reagent (Invitrogen) and purified with the RNeasy Plus kit (Qiagen, Valencia, CA, USA). The quality and concentration of RNA were determined by spectrophotometry (OD at 260 nm) with a Nanodrop. Total RNA (200 ng) was reverse-transcribed in a 20-μl final reaction volume using the high-capacity cDNA reverse transcription kit with RNase inhibitor (Applied Biosystems, Paris, France, USA) following the manufacturer's instructions. qPCR reactions were then performed using the 7900HT real-time PCR system (Applied Biosystems). The forward and reverse primer sequences were as described previously (30): Utrophin-A forward, 5′-ACGAATTCAGTGACATCATTAAGTCC; Utrophin-B forward, 5′-CAGGCTTGCAGGAGATCCC; Utrophin-A and -B reverse, 5′-ATCCATTTGGTAAAGGTTTTCTTCTG. Each primer pair was tested, and melt curves were constructed and analyzed to ensure that only a single amplicon was generated. PCR was performed in plates in a final volume of 10 μl, containing Fast SYBR Green Master Mix, 0.5 μM of each primer, and cDNA corresponding to 0.6 ng of mRNA. Standard PCR conditions were used for the Applied Biosystems assays: 95°C for 20 s and 40 cycles at 95°C for 1 s alternating with 60°C for 25 s. All samples were assayed in duplicate for each target or 6 housekeeping genes, and the averaged values were used as cycle threshold. The most stable housekeeping genes were selected by analyzing results with GeNorm and Normfinder functions in Genex 4.3.8 (MultiD, Göteborg, Sweden). The geometric mean of the 5 best housekeeping genes (GAPDH, HPRT, L32, ACTB, and TUBB) was used to normalize utrophin-A and -B expression levels. Changes in the relative expression of genes of interest were calculated.

Serum CK determination

Blood samples were taken from hearts of anesthetized mice immediately before euthanasia. Serum CK activity was determined using a BioMérieux kit (enzyline CK NAC optimized 10; BioMérieux, Marcy-l'Étoile, France).

Magnetic resonance imaging (MRI)

MRI was performed as described previously in Voisin *et al.* (18). The percentage of normal muscle and necrotic muscle areas was calculated. AMIRA software permitted 3-dimensional (3D) hind-limb reconstruction and 3D visualization of muscle damage.

Masson's trichrome stain

Cryostat muscle sections (7 μm) were stained with Masson's trichrome stain to visualize connective tissue and muscle fibers in pink and collagen in blue (Sigma kit HT15; Sigma-Aldrich) and then observed using a Leica DM RXA2 microscope (Leica Microsystems). The sections were photographed using a CoolSNAP camera (Roper Scientific) and Openlab acquisition software (Improvision).

Evans blue dye

Evan's blue dye (10 mg/ml) in PBS was prepared extemporaneously and filtered through paper (31). A volume of 100 μl/10 g body weight was injected 9 h prior to euthanasia. Diaphragms were excised and digitally photographed for macroscopic evaluation with a binocular magnifying glass equipped with a Canon PowerShot S45 camera (Canon, Tokyo, Japan).

Measurement of ventilation

Breathing activity in adult mice was monitored using the barometric method. The mouse was placed in a plethysmograph chamber (700 ml) and was partially restrained by the tail, with a thin temperature rectal probe. Within the chamber, the animal was positioned in a small rectangular box (4×4×9 cm) opened at both ends, which allowed the animal to reposition itself during the experiment. The chamber was maintained at 27 ± 1°C and was hermetically sealed for 90 s during data collection sessions. Between sessions, the chamber was constantly flushed with fresh humidified air (1 L/min) or with two hypercapnic gas mixtures (6 and 8% CO_2, 21% O_2, balance N_2) administered sequentially for 10 min each. The mice were habituated to the chamber over the previous 2 d. During data collection, tidal volume (V_T) and respiratory frequency (f_R) were continuously recorded. Minute ventilation was then calculated ($V_E = V_T \times f_R$).

Mechanics of isolated muscles

Animals were anesthetized by intraperitoneal injection of a mix of 10 ml/kg of ketamine (10 mg/ml) and xylazine (1 mg/ml), in order to preserve muscle perfusion during dissection of the soleus muscles. The muscle was dissected free from adherent connective tissue and soaked in an oxygenated Krebs solution (95% O_2 and 5% CO_2) containing NaCl (118 mM), $NaHCO_3$ (25 mM), KCl (5 mM), KH_2PO_4 (1 mM), $CaCl_2$ (2.5 mM), $MgSO_4$ (1 mM), and glucose (5 mM) maintained at a temperature of 20°C.

Muscle strips were connected at one end to an electromagnetic puller and at the other end to a force transducer. Stimulation was delivered through electrodes running parallel to the muscle. Tetanic (100 Hz, 500 ms) isometric contractions were studied at L_0 (the optimal length at which maximal tetanic isometric force is observed).

For comparative purposes, normalized isometric force instead of force was assessed. Isometric force was calculated by dividing the force by the estimated cross-sectional area of the muscle. Assuming muscles have a cylindrical shape and a density of 1.06 mg/mm^3, cross-sectional area corresponds to the wet weight of the muscle divided by its fiber length.

Combined forelimb and hind-limb grip strength measurement

Grip strength was measured using a grip strength meter (Bioseb, Vitrolles, France). The apparatus consisted of a grid connected to a digital dynamometer. The animals were gently lowered over the top of the grid so that both sets of front paws and hind paws could grip the grid. While the torso of the animal was kept parallel to the grid, the mouse was gently pulled back by the tail until it released its grip. This procedure was repeated 3 times, and the values were averaged and normalized to mouse body weight.

Inverted grid test

Mice were placed individually on a cage wire grid ~35 cm above a table. After slowly turning the grid through 180°, the length of time the mice continued to grip the grid was

monitored (grip latency), a maximum score of 180 s being given if the animal did not fall. This procedure was repeated 3 times. The values were averaged and normalized to mouse body weight.

In vitro human myotube preparation

Satellite cell populations were isolated as described previously (32) from surgical samples obtained from 4 patients with DMD aged 14 to 25 yr (Banque de Tissus pour la Recherche, Paris, France). After 5 d, when the first mononucleated cells migrated out of the explants, the explants were removed, and the cells were trypsinized (trypsin-EDTA; Invitrogen), collected by centrifugation, and counted. The cell cultures were incubated at 37°C at an initial concentration of 30,000 cells/35-mm-diameter dish, in a humid atmosphere containing 5.5% CO_2. Cultures were grown in a medium consisting of Ham's F-10 supplemented with 20% FCS. After 5 d, growth medium was changed to differentiated medium (Ham's F-10 supplemented with 10% HS). After another 5 d, myotubes were treated with AB (0.1, 0.2, 0.5, 1, and 2 mM) for 48 h. Utrophin expression was determined by Western blot analysis. The histone acetylation state of the myotubes was determined after 48 h of treatment with AB (0.1, 0.5, and 1 mM) or L-arginine (0.066, 0.33, and 0.66 mM) or butyrate (0.034, 0.17, and 0.34 mM).

Statistics

Data are shown as means ± SE and are from ≥3 different experiments. Statistical group comparisons were performed using Student's *t* test with the level of significance set at $P < 0.05$.

RESULTS

In vivo protocol I: continuous-chronic intraperitoneal administration of AB

Utrophin and β*-dystroglycan are up-regulated in muscles from newborn and adult* mdx *mice*

The effects of AB were first evaluated in adult *mdx* mice after 6 series of injections (5 consecutive days per week for 6 wk, at 5 to 300 mg/kg/d). After the treatment, utrophin immunostaining was increased in an apparent dose-dependent manner from 5 to 100 mg/kg/d, reaching comparable levels at the doses of 100 and 200 mg/kg/d (data not shown). We selected the dose of 100 mg/kg/d for the following experiments. Utrophin immunoreactivity appeared in large areas of muscle sarcolemma in gastrocnemius, soleus, tibialis anterior (TA), and diaphragm (**Fig. 1*A***). Utrophin labeling was also increased in the capillaries (Fig. 1*B*). Experiments were also performed in newborn mice with the same protocol (5 d/wk for 6 wk). In newborn mice, utrophin staining at the sarcolemma was weak in TA, soleus, and diaphragm in saline-injected mice, while pronounced staining was obtained after injections of a dose of AB adapted to newborn animals, as determined in a pilot study (25 mg/kg/d AB for 6 wk; Fig. 1*C*).

The putative relocalization of β-dystroglycan, a transmembrane dystrophin-associated protein (33), which is

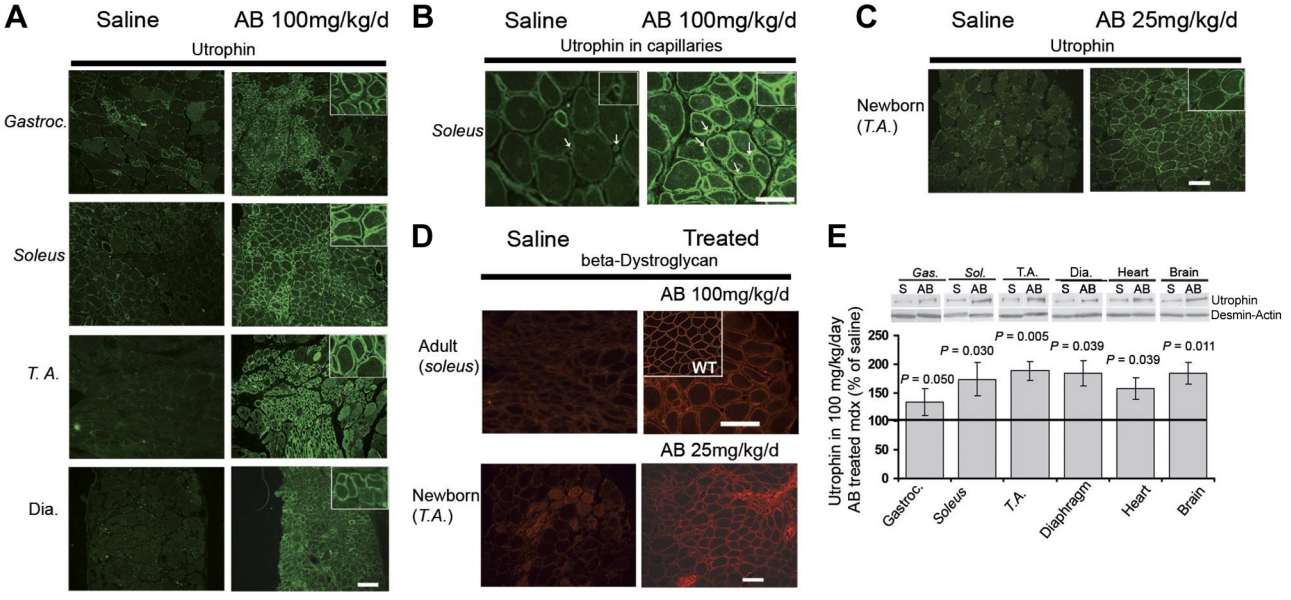

Figure 1. Utrophin in adult and newborn *mdx* mice subjected to the 6-wk continuous-chronic AB treatment protocol. *A*) Utrophin immunostaining in gastrocnemius (gastroc.), soleus, TA, and diaphragm (dia.) of adult *mdx* mice (n=10) after AB treatment (100 mg/kg/d, the dose that produced maximal staining) or saline injections. *B*) Utrophin immunostaining in capillaries of soleus muscle in adult *mdx* mice after AB (100 mg/kg/d) or saline treatments. *C*) Utrophin immunostaining in the TA of *mdx* mice treated from birth with AB (25 mg/kg/d; n=5) compared with the saline group. *D*) β-Dystroglycan immunostaining in soleus muscles of adult *mdx* or WT (inset) mice treated with AB (100 mg/kg/d) and in TA of newborn *mdx* mice treated with AB (25 mg/kg/d). Scale bars = 100 μm. Original view: ×3. *E*) Utrophin levels expressed as a percentage of the level in the saline group were increased in gastrocnemius (gas.; 1.3-fold), soleus (sol.; 1.7-fold), TA (1.9-fold), diaphragm (1.8-fold), heart (1.6-fold), and brain (1.8-fold) in *mdx* mice at the dose of 100 mg/kg/d (n=3/treatment) of AB. Loading controls: desmin for muscle and actin for brain extracts.

not properly integrated into the sarcolemma in patients with DMD, was also assessed. Gastrocnemius, soleus (Fig. 1*D*), TA, and diaphragm muscles of treated adult *mdx* mice showed more pronounced β-dystroglycan staining at the sarcolemma compared with saline-injected mice. Similarly, in treated newborn *mdx* mice, soleus, TA (Fig. 1*D*), and diaphragm muscles showed more pronounced staining for β-dystroglycan as compared with saline-injected mice (dose 25 mg/kg/d).

Semiquantitative Western blot analyses revealed a near 2-fold increase in utrophin expression in the gastrocnemius, soleus, TA, diaphragm, heart, and brain tissues, in *mdx* mice treated with AB at the dose of 100 mg/kg/d (Fig. 1*E*), as compared with mice injected with a saline solution. The relative increase was lower (1.7-fold) at 5 mg/kg/d, whereas no further increase was found at a higher dose of 200 mg/kg/d (data not shown).

Decreased serum CK levels in adult and newborn mdx mice: synergistic effect

In adult *mdx* mice treated with AB at 50 and 100 mg/kg/d, CK level was reduced to about half the level observed in saline-injected *mdx* mice (**Fig. 2*A***), indicating a reduction of muscle necrosis. AB treatment had no effect on CK levels in WT mice injected at 100 mg/kg/d in the same conditions (n=10/treatment group; data not shown). The inverted bell-shaped dose response curve for CK indicated that AB's beneficial effect was obtained from dose 50 mg/kg/d (ratio of 1: a combination that corresponds to 33 mg/kg/d arginine plus 17 mg/kg/d butyrate). The beneficial effect with butyrate (alone) was obtained at 55 mg/kg/d, while the minimal effective dose for arginine (alone) was 200 mg/kg/d, thus demonstrating a synergistic action of arginine and butyrate when used in combination. The effect of AB on CK levels was also evaluated in newborn *mdx* mice. AB reduced CK levels by ~70% compared with saline-injected *mdx* mice at doses of 25, 50, and 60 mg/kg/d (Fig. 2*B*), suggesting that AB treatment was more effective in immature than mature tissues.

Improvement of respiratory function and diaphragm structure in adult mdx mice

In vivo ventilatory function depends on neural control and drive, as well as on blood flow regulation and muscle production. Respiratory function, a major parameter affected in patients with DMD, was, here, evaluated in mice treated with a 100 mg/kg/d dose of AB. The V_T, f_R, and V_E were all lower in control *mdx* mice than in WT mice (**Fig. 3*A***, top panels). During exposure to 6 and 8% CO_2, the V_T was increased in *mdx* mice treated with AB as compared with saline-injected mdx mice. In contrast, the f_R was unaffected. Consequently, the V_E was not modified by treatment (Fig. 3*A*, bottom panels). There was no effect of AB on ventilatory function in WT mice (data not shown).

An enhanced V_T may reflect improved structure of the diaphragm muscle. To confirm this hypothesis, we analyzed the extent of diaphragm necrosis using Evan's blue dye, a vital stain used to identify areas of necrosis and cell damage. We found so few fibers stained by Evan's blue dye in diaphragm from treated *mdx* mice that we considered that quantification was not justified (Fig. 3*B*). Infiltration of diaphragm by collagen, another marker of tissue damage, was visualized using Masson's trichrome stain. As shown in Fig. 3*C*, *mdx* mice treated with AB displayed reduced collagen infiltration (stained blue) in the diaphragm along with improved myofiber organization.

Improvement of hind-limb muscle structure and function in adult mdx *mice*

The body weight of adult *mdx* mice receiving continuous-chronic AB administration increased modestly (~10%) at

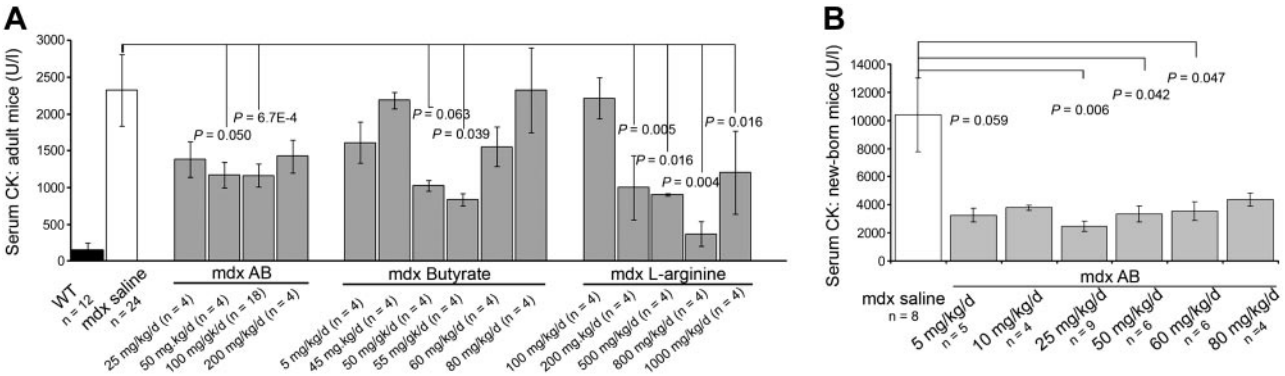

Figure 2. Serum CK level in adult and newborn *mdx* mice subjected to the 6-wk continuous-chronic AB treatment protocol. *A*) Adult untreated *mdx* mice exhibited high levels of serum CK activity (2322±312 U/L) compared with WT mice (153±100 U/L). However, serum CK levels decreased to 40–50% of those of saline-injected *mdx* mice after treatment with AB at 50 and 100 mg/kg/d. AB dose of 50 mg/kg/d corresponds to 33 mg/kg/d of L-arginine plus 17 mg/kg/d of butyrate, while reduction of CK with L-arginine was obtained from dose of 200 mg/kg/d and with butyrate from dose of 55 mg/kg/d, demonstrating a synergistic action of both drugs when used in combination. *B*) Newborn serum CK levels decreased to 70% of those of saline-injected *mdx* mice when the *mdx* mice were injected from birth from 25 to 60 mg/kg/d. Reduction of CK was nearly significant at a dose of 5 mg/kg/d (P=0.059).

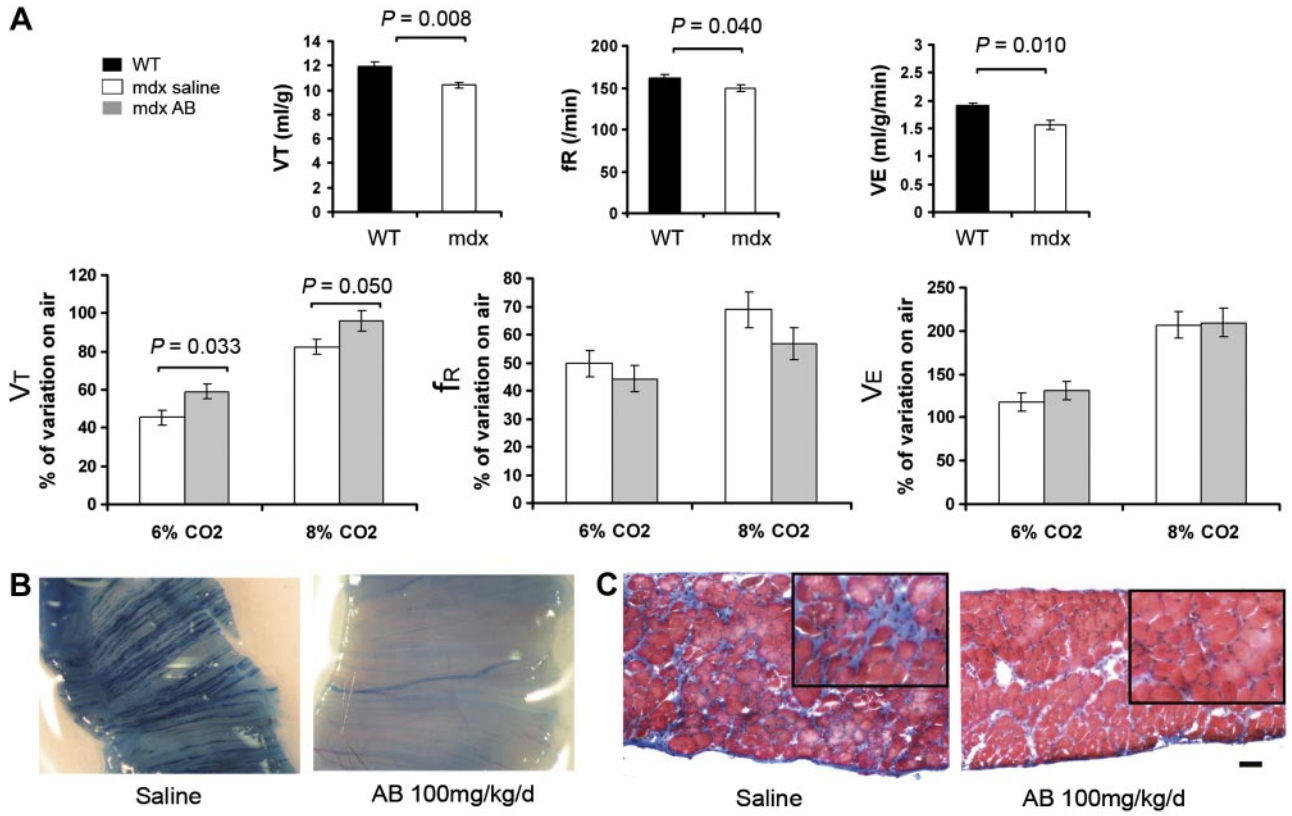

Figure 3. Improved respiratory function and diaphragm muscle structure in *mdx* mice subjected to the 6-wk continuous-chronic AB treatment protocol (100 mg/kg/d). *A*) Top panels: basal ventilatory function at rest in *mdx* mice and WT mice (n=10/group). During exposure to room air, V_T, f_R, and V_E ($V_T \times f_R$) were reduced by 13, 7.5, and 20%, respectively, in *mdx* compared with WT mice. Bottom panels: ventilatory function in adult-treated and saline-injected *mdx* mice (n=10/group) was assessed when muscles were strongly solicited under hypercapnic conditions (6 and 8% CO_2). During hypercapnia, V_T showed a greater increase (14% more) in AB-treated than in saline-injected *mdx* mice. The f_R and, consequently, V_E were not modified. *B*) Reduction of necrosis in the diaphragm after treatment with AB, as demonstrated by the exclusion of Evans's blue dye from the treated muscle, as compared with saline. Diaphragm of saline-injected *mdx* mice (n=3) had numerous necrotic fibers, as evidenced by extensive areas stained by Evan's blue dye. In contrast, necrotic fibers were almost absent in *mdx* mice (n=5) after AB injections. *C*) Masson's trichrome staining of diaphragm in untreated *vs.* treated *mdx* mice (n=6). AB treatment in *mdx* mice reduced the amount of collagen infiltration (stained in blue) in the diaphragm compared with untreated mice. Scale bar = 50 μm. Original view: ×3.

doses 50, 100, and 200 mg/kg/d as compared with saline-injected mice (Supplemental Fig. S1*A*). This was associated with an increased weight of TA and soleus muscles (Supplemental Fig. S1*B*), but not of gastrocnemius.

An MRI study was performed in *mdx* mice before (T_0) and after (T_0+6 wk) treatment with AB (100 mg/kg/d), providing an *in situ* evaluation of muscle necrotic areas in living animals. Reduced necrosis was readily visible in tissue sections (**Fig. 4*A***) and in 3D reconstitutions of the hind limb (Fig. 4*B*), and the quantification of the necrotic areas confirmed the significant reduction in *mdx* mice treated with AB compared with those injected with a saline solution (Fig. 4*C*). As shown in Fig. 4*D*, this was associated with reduced fibrosis and improved structure of the hind-limb muscles, which more closely resembled healthy tissue (as illustrated for the soleus muscle in the figure).

To document further the alleviation of myopathy by AB treatment, we measured the isometric force in soleus muscles of *mdx* mice injected with AB or NaCl. *Mdx* mice treated with AB showed a 23% increase in the isometric force (n=19 muscles), as compared with saline-injected *mdx* mice (n=13 muscles). Although this improvement was statistically significant (P<0.03), the isometric force in treated *mdx* mice did not reach the levels of healthy WT mice (n=8 muscles; Fig. 4*E*).

In vivo protocol II: intermittent intraperitoneal AB_{cf} administration

In this series of experiments with adult mice, the frequency of injections was reduced, and preliminary experiments demonstrated that higher doses could then be used. The AB formulation used in this protocol was different to that used in the previous experiments: it was based on the formulation recently applied in patients suffering from β-globin disorders, *i.e.*, it corresponded to a 0.76 M arginine instead of 1 M. This distinct formulation is referred to as AB_{cf} in all parts of the text and in the figures.

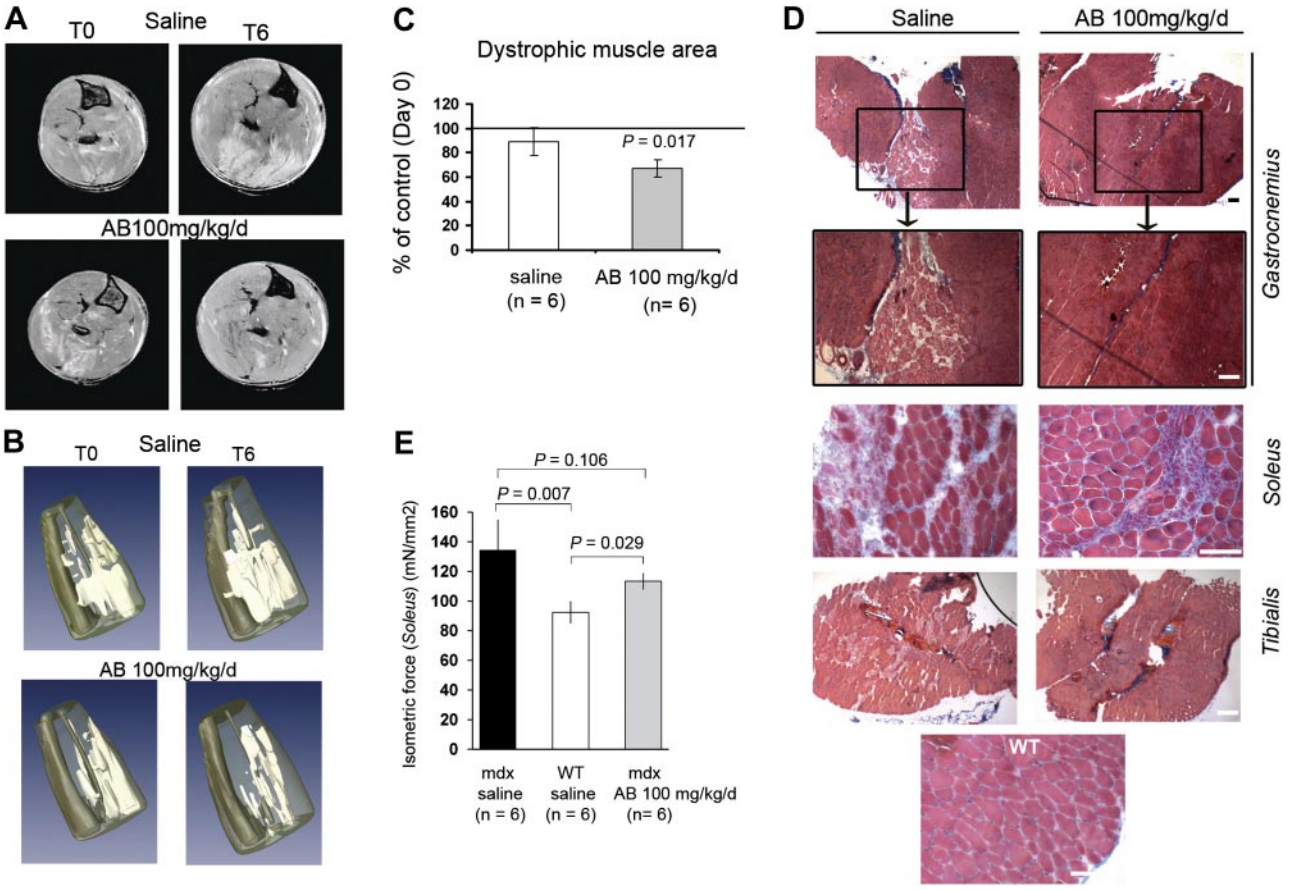

Figure 4. Muscle structure and function in adult *mdx* mice subjected to the 6-wk continuous-chronic AB treatment protocol (100 mg/kg/d). *A*) Lower limbs of adult *mdx* mice were examined by cross-sectional MRI before (T_0) and after [T_0+6 wk (T_6)] treatment with saline solution or AB (n=6/case). Black, bone cavities; white, fat and damaged tissues; gray, healthy muscle tissue. For each animal, the percentage of areas containing healthy muscle (gray) and damaged muscle (white) were measured in 4 consecutive slices corresponding to the median part of the hind limb, at T_0 and T_6 (subcutaneous fat was excluded). A large decrease in damaged tissue areas was observed after treatment. *B*) Amira-3D reconstitution data analysis enabled visualization of the reduction of necrotic zones in the whole hind limb (brown, bone; white, damaged tissues). *C*) Quantification of necrotic surfaces from MRI study; results are presented as percentages of control (d 0). A large reduction of necrotic areas (30%) was observed after treatment with AB. *D*) Masson's trichrome staining of gastrocnemius (original view: ×2), soleus, and tibialis anterior (TA) in untreated *vs.* treated mice (n=10/treatment). Muscles from saline-injected *mdx* mice had extensive areas of necrosis characterized by extensive areas of connective tissue invasion. Following AB treatment, the muscle more closely resembled healthy tissue (WT; illustrated: soleus muscle). Scale bars = 250 μm. *E*) Isometric force production. Isometric force was slightly (23%) increased in soleus muscles of treated *mdx*, compared with untreated mice.

Series of 4 injections (every 2 wk for 6 wk)

The body weight of *mdx* mice treated for 4 consecutive days every 2 wk for 6 wk (3 series of injections) increased by up to 21% at doses from 500 to 1000 mg/kg/d (Supplemental Fig. S1*C*), which is greater than the changes induced by continuous-chronic injections (~10%). No change in body weight was detected in WT mice (data not shown).

An effect of AB_{cf} on muscle strength was first evaluated using a grip-strength meter. AB_{cf} treatment improved *mdx* mice grip strength at doses 600 and 800 mg/kg/d in a dose-dependent manner (**Fig. 5*A***). In the inverted grid test, the ability of AB_{cf}-treated *mdx* mice to maintain a grip on an inverted grid (grip latency) varied according to mice but was significantly improved at the dose of 600 mg/kg/d (Fig. 5*B*).

Intermittent treatment with AB_{cf} also significantly reduced the serum CK levels at doses of 200, 500, 600, 800, and 1000 mg/kg (Fig. 5*C*). However, CK levels in AB_{cf}-treated *mdx* mice never reached the very low levels that are typically measured in the WT mice, thus showing again that AB alleviates myopathy but does not lead to complete rescue of the dystrophic phenotype. Increasing the interval between the series of 4 daily injections from 2 to 3 wk (2 series of injections during the 6 wk of the protocol) induced a reduction of CK levels of ~30% in *mdx* mice treated with the higher doses (600, 800, and 1000 mg/kg/d), though this group difference did not reach statistical significance (data not shown).

Western blot analyses showed that in TA muscle, AB_{cf} increased expression levels of utrophin at doses of 200, 600, 800, and 1000 mg/kg/d (EC_{50}=284 mg/ml; Fig.

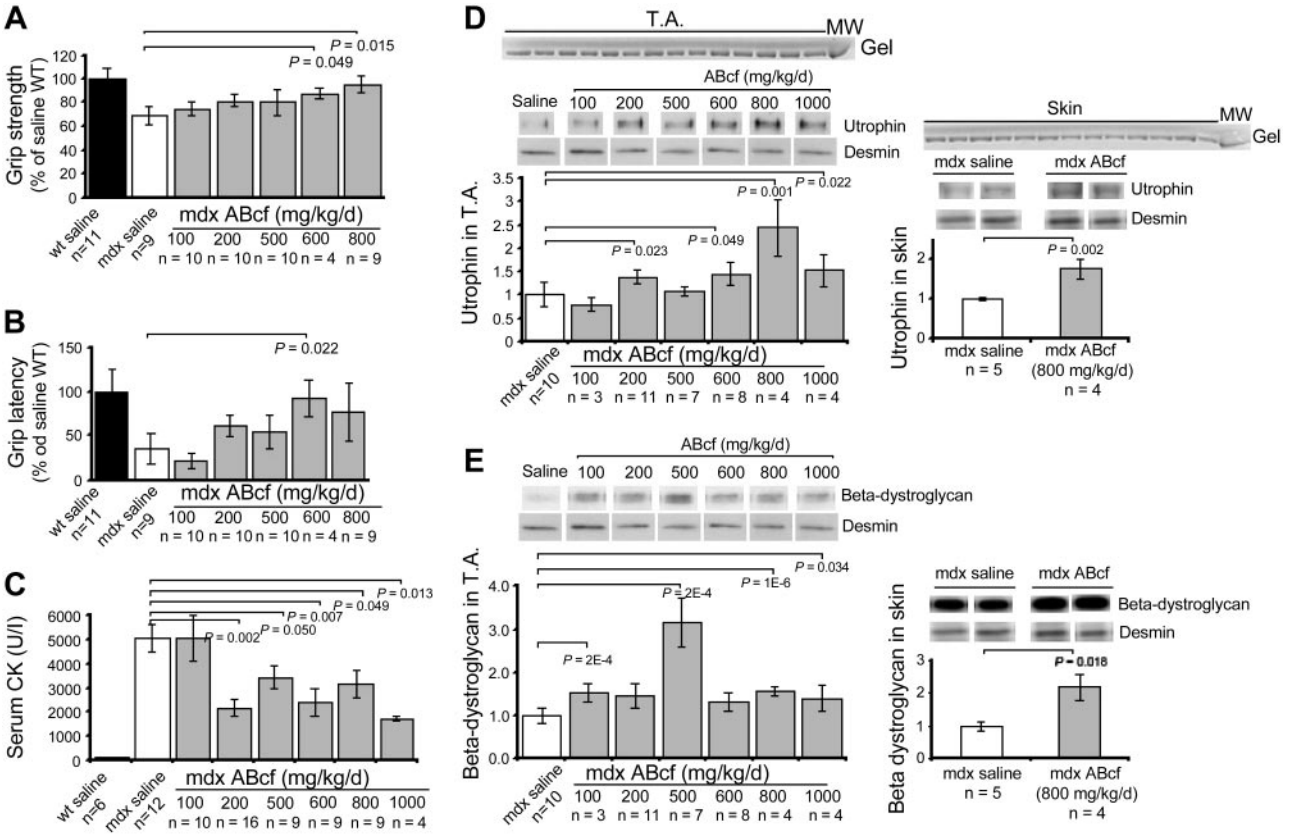

Figure 5. Beneficial effects of AB_{cf} (100 to 1000 mg/kg/d) administered to adult *mdx* mice for 6 wk following an intermittent protocol. *A*) Grip strength of saline-injected *mdx* mice was 70% of that of WT mice. AB_{cf} treatment (100–800 mg/kg/d) at doses of 600 and 800 mg/kg/d improved *mdx* mouse grip strength, which reached 88 and 95% of the WT value, respectively. *B*) In the inverted grid test, grip latency in WT mice was 3-fold longer than in the saline-injected *mdx* mice. Treatment at 600 mg/kg/d improved grip latency, which reached 92% of the WT value. *C*) AB_{cf} treatment reduced serum CK levels by ~50% at doses of 200 to 1000 mg/kg as compared with saline. *D*, *E*) Utrophin (*D*) and β-dystroglycan (*E*) expression was assessed by Western blot in TA muscle of *mdx* mice receiving 100 to 1000 mg/kg/d of AB_{cf}. Equal loading was verified by staining protein gels with Coomassie blue (MW, molecular weight marker). Graph shows the mean values for ≥3 different experiments. Results were normalized to saline values (treated/saline ratio). Values are representative of 3 independent experiments. *D*) Utrophin expression level was increased in TA from treated mice compared with saline-injected mice at 200 (1.9-fold), 600 (1.45-fold), 800 (2.45-fold), and 1000 (1.5-fold) mg/kg/d. In skin from mice injected with AB_{cf} at 800 mg/kg/d, utrophin levels were increased 1.8-fold compared with saline. *E*) β-Dystroglycan levels were increased in TA from treated mice at 100 (1.5-fold), 500 (3-fold), 800 (1.6-fold), and 1000 (1.4-fold) mg/kg/d. In skin samples, β-dystroglycan expression level was increased 1.7-fold at 800 mg/kg/d as compared with saline. Increased utrophin and β-dystroglycan expression levels in soleus are shown in Supplemental Fig. S2.

5*D*) and that of β-dystroglycan at doses of 100, 500, 800, and 1000 mg/kg/d (Fig. 5*E*). In the soleus, utrophin (at doses of 800 and 1000 mg/kg/d) and β-dystroglycan (at doses of 200, 500, 600, and 1000 mg/kg/d) were also overexpressed (Supplemental Fig. S2). Moreover, we also showed that AB_{cf} could increase utrophin expression in mouse skin samples (Fig. 5*D, E*), reflecting widespread effects of AB in various tissues and organs and raising the possibility of using skin biopsies to monitor treatment effects over time.

One single series of 4 injections of AB_{cf}

In a clinical trial, a biopsy performed shortly after the beginning of the treatment could be useful to validate the first expected effect of AB_{cf} in muscles of the patient, *i.e.*, an increase in expression of utrophin and associated proteins, such as β-dystroglycan or embryonic myosin (a putative marker of regeneration). In anticipation of the biopsies that could be scheduled in clinical trials, we determined the time frame in which utrophin expression could be clearly up-regulated in muscle tissues from treated *mdx* mice. Mice were sacrificed 24 h after a single series of 4 consecutive daily injections (d 5) or 1 wk later (d 12).

Expression of utrophin, β-dystroglycan, and embryonic myosin was analyzed by Western blot in the same muscle extracts. Utrophin expression was increased 24 h after the end of the treatment in the TA of *mdx* mice treated with AB_{cf} at 800 mg/kg/d (**Fig. 6*A***). This overexpression of the utrophin protein was associated with an increased expression of utrophin-A mRNA, as evaluated by qPCR (Fig. 6*B*). No increases were observed for the utrophin-B mRNA level (ratio: 0.93±0.019, range: 0.88–1.10; $P>0.05$; data not shown)

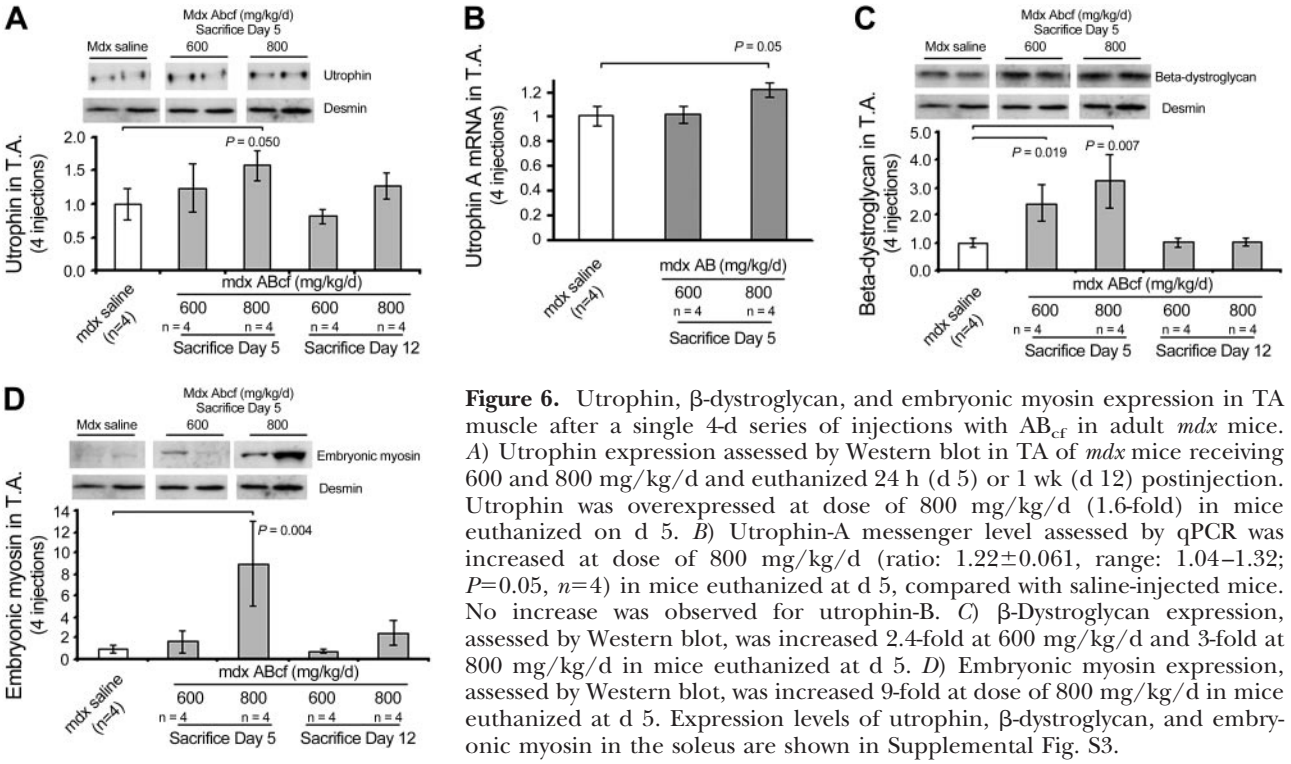

Figure 6. Utrophin, β-dystroglycan, and embryonic myosin expression in TA muscle after a single 4-d series of injections with AB_{cf} in adult *mdx* mice. *A*) Utrophin expression assessed by Western blot in TA of *mdx* mice receiving 600 and 800 mg/kg/d and euthanized 24 h (d 5) or 1 wk (d 12) postinjection. Utrophin was overexpressed at dose of 800 mg/kg/d (1.6-fold) in mice euthanized on d 5. *B*) Utrophin-A messenger level assessed by qPCR was increased at dose of 800 mg/kg/d (ratio: 1.22±0.061, range: 1.04–1.32; P=0.05, n=4) in mice euthanized at d 5, compared with saline-injected mice. No increase was observed for utrophin-B. *C*) β-Dystroglycan expression, assessed by Western blot, was increased 2.4-fold at 600 mg/kg/d and 3-fold at 800 mg/kg/d in mice euthanized at d 5. *D*) Embryonic myosin expression, assessed by Western blot, was increased 9-fold at dose of 800 mg/kg/d in mice euthanized at d 5. Expression levels of utrophin, β-dystroglycan, and embryonic myosin in the soleus are shown in Supplemental Fig. S3.

β-dystroglycan expression levels were significantly increased at doses of 600 and 800 mg/kg/d in tissues analyzed 24 h after the end of treatment (Fig. 6*C*). Expression of embryonic myosin was strongly increased at 800 mg/kg/d 24 h after the end of treatment (Fig. 6*D*). Similarly in the soleus, utrophin, and β-dystroglycan, expression levels were increased 24 h after the end of treatment in *mdx* mice treated with AB_{cf} at 800 mg/kg/d (Supplemental Fig. S3*A*, *B*), while expression of embryonic myosin was increased at both 600 and 800 mg/kg/d (Supplemental Fig. S3*C*). Utrophin and β-dystroglycan immunostaining revealed localization in the soleus sarcolemma, and the staining for embryonic myosin was strongly increased in treated mice (Supplemental Fig. S4).

However, in both TA and soleus muscles, none of these changes were maintained when mice were sacrificed 1 wk after the fourth injections, thus confirming the need for a chronic regimen to maintain the effects of AB.

Interestingly, utrophin and β-dystroglycan were also overexpressed in the brain of treated *mdx* mice: utrophin protein was overexpressed by 37% (P<0.03) and β-dystroglycan by 74% (P<0.001) at the dose of 800 mg/kg/d, 24 h after the end of treatment. In contrast to the muscle tissues, these changes were persistent, as mice euthanized 1 wk after the fourth injections still showed significant overexpression of utrophin (216%; P=0.001) and β-dystroglycan (200%; P<0.001) (data not shown). This delay could reflect better diffusion of AB in brain tissues due to the blood-brain barrier dysfunction reported in *mdx* mice (34), or unidentified differences in the dynamics of AB metabolism and/or regulation of utrophin expression and stabilization in muscle *vs.* brain tissues.

In vitro AB treatment in human cultured myotubes

How AB affects utrophin expression in human tissue was determined by Western blot analysis of myotube extracts obtained from myoblasts isolated from DMD volunteers. Treatment with 0.1–2 mM AB for 2 d increased utrophin expression around 2-fold in human myotubes (**Fig. 7*A***), in an apparent dose-dependent manner at doses from 0.1 to 1 mM. Localization of utrophin in myotubes was observed after immunostaining of utrophin: little utrophin labeling was visible in untreated myotubes, but staining was slightly increased in the sarcolemma after treatment (Fig. 7*B*). This increase of utrophin in human myotubes suggests that the treatment may have a similar effect in muscles of patients with DMD. In addition, the synergistic effect of AB was also demonstrated by analyzing the chromatin acetylation state in Western blot experiments using an antibody against the acetylated part of histone H3 (Lys 9). An increased acetylation level was expected after treatment with butyrate, due to its histone deacetylase inhibitor properties. This was, however, not directly expected following treatment with L-arginine alone, although recent studies suggest that NO may also be involved in epigenetic histone modification and gene expression regulation in *mdx* mice, as well as in C2C12 myoblasts from patients with DMD (35). Here, human myotubes were treated with different doses of AB or L-arginine or butyrate alone. In a first group, we compared AB (0.1 mM) with the corresponding doses of L-arginine (0.066 mM) or butyrate (0.034 mM) alone; in a second group, we compared AB (0.5 mM) with the corresponding doses of L-arginine (0.33 mM) or butyrate (0.17 mM) alone; and in a last group, we com-

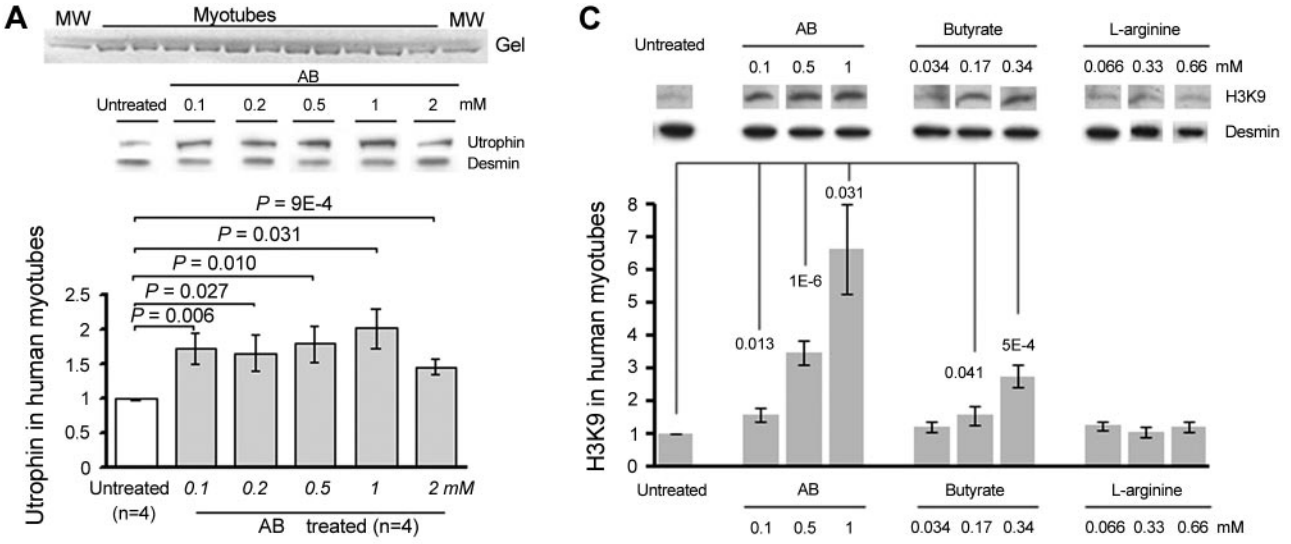

Figure 7. Primary cultures of myotubes prepared from DMD patient myoblasts under control conditions (untreated) and after 48-h treatment with AB, L-arginine, or butyrate. Utrophin analysis after treatment with AB. *A*) For immunoblot analyses, equal loading was verified by staining protein gels with Coomassie blue (MW, molecular weight marker). Graph shows the mean values for ≥3 different experiments. Results are expressed as treated/untreated ratios. Values are representative of 3 independent experiments. Utrophin level was increased (~2-fold) after treatment with AB (0.1–2 mM). *B*) For immunostaining, little staining was observed in untreated myotubes, but utrophin was clearly detected under the sarcolemma in treated myotubes (AB, 0.5 mM). Scale bar = 68 μm. *C*) Level of histone H3 acetylated at Lys 9 (H3K9) after treatment with AB, L-arginine, and butyrate. Results are expressed as treated/untreated ratios. Values are representative of 3 independent experiments. H3 acetylation levels were increased in myotubes treated with AB (0.5–1 mM; 2- to 6-fold) or with butyrate (0.034–0.34 mM; 1.5- to 3-fold), but not with L-arginine (0.066–0.66 mM). Note the dose-dependent effect of AB and butyrate on H3 acetylation level.

pared AB (1 mM) with the corresponding doses of L-arginine (0.66 mM) or butyrate (0.34 mM) alone. A dose-dependent increase in the acetylation of histones was observed following treatment with AB and butyrate (Fig. 7*C*), which is reminiscent of the effects on utrophin expression level (Fig. 7*A*). In contrast, L-arginine alone did not induce any chromatin change. When myotubes were treated with 0.1 mM AB the level of acetylation was increased, while this was not observed with the corresponding doses of L-arginine (0.066 mM) or butyrate (0.034 mM) alone. Similarly, with 0.5 mM AB the level of acetylation was strongly increased, not with the corresponding doses of L-arginine alone (0.33 mM) and only modestly with butyrate alone (0.17 mM). The same tendency was obtained with 1 mM AB compared with the corresponding doses of L-arginine (0.66 mM) and butyrate (0.34 mM). These results demonstrate a synergistic effect of arginine and butyrate on chromatin acetylation level when used in combination.

DISCUSSION

In the present study, arginine and butyrate were associated in a salt in two distinct but close formulations, AB and AB_{cf}, and tested for preclinical efficacy as a potential treatment option for patients with DMD. Previous studies have demonstrated the beneficial effects of arginine (11, 12, 14, 15, 18, 19) and of histone deacetylase inhibitors [trichostatin (25) and valproic acid (26)] used separately in *mdx* mice. Besides, recently published results support the clinical use of AB in pediatric patients (29, 36–39).

In our experimental setting, chronic continuous treatment of *mdx* mice with AB for 6 wk induced an up-regulation of utrophin expression in skeletal muscles, heart, brain, and skin. Utrophin overexpression was associated with dose-dependent beneficial effects on the dystrophic phenotype.

In *mdx* mice, as in patients with DMD, the mRNAs of dystrophin-associated protein (DAP) and dystrophin-associated glycoprotein (DAG) complexes are expressed at normal levels. However, in the absence of dystrophin, these proteins are no longer integrated into the sarcolemma and are subsequently degraded, leading to a reduction of DAGs and DAPs in muscle tissues (40). Our results indicate that utrophin and β-dystroglycan are properly localized to the sarcolemma after AB treatment, suggesting that the treatment may be sufficient to restore sarcolemmal integrity.

This is supported by the associated decreases in serum CK levels and the incorporation of Evans blue dye in myofibers. The bell-shaped dose response curve demonstrated by body weight index is mirrored by the inverted bell shape of CK release. Changes in CK level indicate a beneficial effect obtained from the dose of 50 mg/kg/d with AB (33 mg/kg/d arginine plus 17 mg/kg/d butyrate), from the dose of 200 mg/kg/d with L-arginine alone and from the dose of 55 mg/kg/d with butyrate alone, as expected in a multiple-targeting situation. These results demonstrate synergistic effects of a low-dose combination of arginine and butyrate, and they support the effectiveness of a combination treatment regimen for the management of patients with DMD, minimizing potential adverse events. In our MRI study, we observe a decrease in both necrosis and proliferation of connective tissue in AB-treated *mdx* mice. Necrosis and extensive proliferation of connective tissue in skeletal muscles are characteristics in human DMD, and treatment with AB may be expected to induce a similar improvement in patients. The MRI analysis provides anatomical evidence of an improved phenotype by a noninvasive procedure, which may also be useful in clinical settings where tissue biopsies cannot be readily obtained. All of these results have been confirmed by Masson's trichrome staining and measurement of the isometric force in excised muscles.

Respiratory function is compromised in *mdx* mice compared with WT mice. However, we show here that AB can improve tidal volume capacity, possibly through a direct effect on the diaphragm, as suggested by the associated decrease in the density of necrotic fibers and connective tissue invasion in this muscle. This suggests that AB could have a positive effect on the respiratory symptoms in patients with DMD.

To further evaluate whether AB may be used for the early treatment of DMD in pediatric patients, we also studied its effects in newborn *mdx* pups. After slight dose adjustments, the results in the males were similar to those found in adult animals. Therefore, it is anticipated that early treatment with AB in pediatric patients with DMD could be well tolerated and might protect muscles against deterioration. Moreover, AB treatment improved muscle function in *mdx* mice as assessed by measurement of isometric force, thus showing that AB does not solely reduce biochemical alterations and improve the structure of muscle tissues, but also leads to substantial improvement in the physiological functions of muscle.

Increases in utrophin expression in other tissues, such as heart and brain could also have positive consequences. It is known that although the lack of dystrophin results in mild cardiomyopathy in *mdx* mice (41), the chronic treatment with L-arginine was shown to ameliorate cardiac function and to reduce necrosis in the heart in *mdx* mice (15). In patients with DMD, the heart can be severely affected, resulting in degeneration of the myocardium, heart failure, and sudden death in 10–30% of patients (42, 43). We also noted an up-regulation of utrophin in the brain of treated *mdx* mice, suggesting that AB may compensate, at least partially, for the lack of brain dystrophin and potentially ameliorate some of the brain and cognitive abnormalities associated with DMD (44). However, we recently showed that this does not overcome behavioral alterations in *mdx* mice (45). This lack of effects in brain is potentially linked to the cellular expression profiles of utrophin and dystrophin, which do not seem to overlap any more in adult brain tissues, unlike their expression in muscle fibers. However, one may hypothesize that AB could have a greater impact when administered to younger mice, when developmental plasticity is still occurring in the immature brain. Moreover, the increased expression of utrophin in the brain is in favor of a direct effect of AB on the mechanisms regulating utrophin expression. This suggests that, in general, the effects of AB are not indirect, such as the differentiation of myoblasts during regeneration processes. Because overexpression of utrophin in a broad range of nonmuscle tissues in transgenic *mdx* mice is not detrimental (46), the use of AB is expected to be a safe therapeutic approach, even if utrophin regulation by this treatment is not tissue-specific.

To be closer to conditions of use of the product in clinical trials, we also evaluated an intermittent protocol that reduces the frequency of injections. This protocol has been developed and applied in clinical trials to treat patients with β-globin disorders. In *mdx* mice, we found that this administration regimen elicits dose-dependent beneficial effects similar to those with the continuous-chronic protocol of injections. This includes changes in utrophin and β-dystroglycan expression, reduction of serum CK levels, and partial increase in muscle strength and alleviation of fatigue. This intermittent protocol also has the advantage of allowing better tolerability at high doses. Indeed, while continuous-chronic injections of AB_{cf} at the dose of 300 mg/kg/d led to a decrease in body weight, suggesting suboptimal tolerability of the product, such detrimental effects were not observed with the intermittent protocol up to a dose of 1000 mg/kg/d. After treatment with high doses of AB, the loss of beneficial effects on body weight (Supplemental Fig. S1*A*) and on CK level (Fig. 2*B*) might explain the modest beneficial effects reported in an initial study performed in *mdx* mice with 250 mg/kg/d of AB (27). Indeed, the optimal dose selected in the current study for chronic-continuous injections was only 100 mg/kg/d. Another explanation could be that the treatment in our initial study (27) was prolonged for several months, which could have induced tolerance to the effects of AB, thus making prolonged treatment ineffective. Other factors could also be responsible for the differences between the two studies, including differences in the age of the animals at the start of treatment. In the present study, mice were aged 8 wk, which is a reliable time to induce treatment since *mdx* mice display important necrosis and regeneration cycles at this age, while in the former study mice were aged 12 wk at the start of treatment. Sex could also be a misleading factor; using only males

reduces variability and better reflects the human condition as DMD affects boys, and sexual dimorphism has been shown in the *mdx* line (47).

A single series of 4 injections of AB_{cf} was sufficient to overexpress utrophin (both protein and mRNA expression), β-dystroglycan, and embryonic myosin in adult *mdx* mice. Thus, in the course of clinical trials using AB_{cf} in humans, biopsies could be performed shortly after the beginning of the treatment, and utrophin expression could be used as a biochemical marker of treatment efficacy. Utrophin is also expressed in the smooth muscle of skin (arrector pili muscle; ref. 48), and we found that AB_{cf} treatment increases utrophin and β-dystroglycan expression in the skin of *mdx* mice, which opens the possibility of easily monitoring utrophin induction in patients along with diagnosis of myopathy using skin samples (49), which could limit the frequency of the more invasive muscle biopsies. The proportion of centronucleated fibers (75% in *mdx* mice) was not reduced in soleus and TA after treatment (data not shown). This result suggests cell replication and muscle regeneration continued at least up to the time at which the mice were sacrificed and is supported by the increase of embryonic myosin observed in treated mice. Increased expression of embryonic myosin may reflect a regeneration process, which is in line with the effects of L-arginine on the activation of satellite cells during muscle repair after injury (50). Unlike previous studies (27, 45), in which no quantitative changes in utrophin mRNA expression were detected, we found here that utrophin-A mRNA was up-regulated in skeletal muscle of treated *mdx* mice. The reasons for this discrepancy could be linked to the assessment of mRNA expression several weeks or months after the start of the product administration. Here, the level of utrophin mRNA was measured after a single series of 4 injections of AB_{cf} and with a 24-h delay after the last injection.

Finally, the beneficial effect on the animal's body weight suggests that AB and AB_{cf} are well tolerated by *mdx* mice, which is consistent with the anabolic effect of L-arginine on muscles (51). Moreover, we show that AB increases utrophin expression in human myotubes, with correct localization at the sarcolemma, suggesting that the beneficial effects of utrophin up-regulation on muscle structure and function could also be achieved in patients with DMD. A comparison of the chromatin acetylation state in human myotubes treated with L-arginine, butyrate, and AB confirmed that the combined formula of AB acts synergistically, as observed in the measurements of CK serum levels *in vivo*. Taken together, our data suggest that AB is a good candidate for systemic up-regulation of utrophin in DMD and deserves to be tested as a proof of concept in clinical trials. FJ

The authors thank Francesca Consolaro for technical assistance for the experiments on the chromatin acetylation state. The authors thank the French Banque de Tissus pour la Recherche (BTR; Institut de Myologie) for providing surgical residues of human paravertebral striated muscles. BTR is a partner of the EuroBioBank network funded by the European Community under the Fifth Framework Program (QLRI-CT-2002-02769). The authors thank M. Bonora (Paris) for help with the respiration protocols and the Imagif qPCR platform. This work was supported by the Association Française contre les Myopathies (2004.001/10689, 2007.1563/12507, 2008.0797/13466); and the Muscular Dystrophy Association (MDA3561, MDA4078). The authors declare no conflicts of interest.

REFERENCES

1. Fairclough, R. J., Bareja, A., and Davies, K. E. (2011) Progress in therapy for Duchenne muscular dystrophy. *Exp. Physiol.* **96,** 1101–1113
2. Voisin, V., and de la Porte, S. (2004) Therapeutic strategies for Duchenne and Becker dystrophies. *Int. Rev. Cytol.* **240,** 1–30
3. Love, D. R., Hill, D. F., Dickson, G., Spurr, N. K., Byth, B. C., Marsden, R. F., Walsh, F. S., Edwards, Y. H., and Davies, K. E. (1989) An autosomal transcript in skeletal muscle with homology to dystrophin. *Nature* **339,** 55–58
4. Karpati, G., Carpenter, S., Morris, G. E., Davies, K. E., Guerin, C., and Holland, P. (1993) Localization and quantitation of the chromosome 6-encoded dystrophin-related protein in normal and pathological human muscle. *J. Neuropathol. Exp. Neurol.* **52,** 119–128
5. Rafael, J. A., Tinsley, J. M., Potter, A. C., Deconinck, A. E., and Davies, K. E. (1998) Skeletal muscle-specific expression of a utrophin transgene rescues utrophin-dystrophin deficient mice. *Nat. Genet.* **19,** 79–82
6. Tinsley, J. M., Potter, A. C., Phelps, S. R., Fisher, R., Trickett, J. I., and Davies, K. E. (1996) Amelioration of the dystrophic phenotype of mdx mice using a truncated utrophin transgene. *Nature* **384,** 349–353
7. Tinsley, J., Deconinck, N., Fisher, R., Kahn, D., Phelps, S., Gillis, J. M., and Davies, K. (1998) Expression of full-length utrophin prevents muscular dystrophy in *mdx* mice. *Nat. Med.* **4,** 1441–1444
8. Chaubourt, E., Fossier, P., Baux, G., Leprince, C., Israel, M., and De La Porte, S. (1999) Nitric oxide and L-arginine cause an accumulation of utrophin at the sarcolemma: a possible compensation for dystrophin loss in Duchenne muscular dystrophy. *Neurobiol. Dis.* **6,** 499–507
9. Chaubourt, E., Voisin, V., Fossier, P., Baux, G., Israel, M., and De La Porte, S. (2002) Muscular nitric oxide synthase (muNOS) and utrophin. *J. Physiol. Paris* **96,** 43–52
10. Anderson, J. E., and Vargas, C. (2003) Correlated NOS-Imu and myf5 expression by satellite cells in mdx mouse muscle regeneration during NOS manipulation and deflazacort treatment. *Neuromuscul. Disord.* **13,** 388–396
11. Archer, J. D., Vargas, C. C., and Anderson, J. E. (2006) Persistent and improved functional gain in mdx dystrophic mice after treatment with L-arginine and deflazacort. *FASEB J.* **20,** 738–740
12. Barton, E. R., Morris, L., Kawana, M., Bish, L. T., and Toursel, T. (2005) Systemic administration of L-arginine benefits *mdx* skeletal muscle function. *Muscle Nerve* **32,** 751–760
13. Brunelli, S., Sciorati, C., D'Antona, G., Innocenzi, A., Covarello, D., Galvez, B. G., Perrotta, C., Monopoli, A., Sanvito, F., Bottinelli, R., Ongini, E., Cossu, G., and Clementi, E. (2007) Nitric oxide release combined with nonsteroidal antiinflammatory activity prevents muscular dystrophy pathology and enhances stem cell therapy. *Proc. Natl. Acad. Sci. U. S. A.* **104,** 264–269
14. Chazalette, D., Hnia, K., Rivier, F., Hugon, G., and Mornet, D. (2005) α7B integrin changes in mdx mouse muscles after L-arginine administration. *FEBS Lett.* **579,** 1079–1084
15. Hoey, A. J., and Erp, C. V. (2006) Effect of L-arginine on cardiac function and fibrosis in *mdx* mice. *Proc. Aust. Physiol. Soc.* **37,** 57
16. Marques, M. J., Luz, M. A., Minatel, E., and Neto, H. S. (2005) Muscle regeneration in dystrophic mdx mice is enhanced by isosorbide dinitrate. *Neurosci. Lett.* **382,** 342–345
17. Segalat, L., Grisoni, K., Archer, J., Vargas, C., Bertrand, A., and Anderson, J. E. (2005) CAPON expression in skeletal muscle is regulated by position, repair, NOS activity, and dystrophy. *Exp. Cell. Res.* **302,** 170–179

18. Voisin, V., Sebrie, C., Matecki, S., Yu, H., Gillet, B., Ramonatxo, M., Israel, M., and De la Porte, S. (2005) L-arginine improves dystrophic phenotype in mdx mice. *Neurobiol. Dis.* **20,** 123–130
19. Hnia, K., Gayraud, J., Hugon, G., Ramonatxo, M., De La Porte, S., Matecki, S., and Mornet, D. (2008) L-arginine decreases inflammation and modulates the nuclear factor-κB/matrix metalloproteinase cascade in mdx muscle fibers. *Am. J. Pathol.* **172,** 1509–1519
20. Benabdellah, F., Yu, H., Brunelle, A., Laprevote, O., and De La Porte, S. (2009) MALDI reveals membrane lipid profile reversion in *MDX* mice. *Neurobiol. Dis.* **36,** 252–258
21. Thomas, G. D., Sander, M., Lau, K. S., Huang, P. L., Stull, J. T., and Victor, R. G. (1998) Impaired metabolic modulation of alpha-adrenergic vasoconstriction in dystrophin-deficient skeletal muscle. *Proc. Natl. Acad. Sci. U. S. A.* **95,** 15090–15095
22. Sander, M., Chavoshan, B., Harris, S. A., Iannaccone, S. T., Stull, J. T., Thomas, G. D., and Victor, R. G. (2000) Functional muscle ischemia in neuronal nitric oxide synthase-deficient skeletal muscle of children with Duchenne muscular dystrophy. *Proc. Natl. Acad. Sci. U. S. A.* **97,** 13818–12823
23. Perrine, S. P., Miller, B. A., Faller, D. V., Cohen, R. A., Vichinsky, E. P., Hurst, D., Lubin, B. H., and Papayannopoulou, T. (1989) Sodium butyrate enhances fetal globin gene expression in erythroid progenitors of patients with Hb SS and beta thalassemia. *Blood* **74,** 454–459
24. Perrine, S. P. (2008) Fetal globin stimulant therapies in the β-hemoglobinopathies: principles and current potential. *Pediatr. Ann.* **37,** 339–346
25. Minetti, G. C., Colussi, C., Adami, R., Serra, C., Mozzetta, C., Parente, V., Fortuni, S., Straino, S., Sampaolesi, M., Di Padova, M., Illi, B., Gallinari, P., Steinkuhler, C., Capogrossi, M. C., Sartorelli, V., Bottinelli, R., Gaetano, C., and Puri, P. L. (2006) Functional and morphological recovery of dystrophic muscles in mice treated with deacetylase inhibitors. *Nat Med* **12,** 1147–1150
26. Gurpur, P. B., Liu, J., Burkin, D. J., and Kaufman, S. J. (2009) Valproic acid activates the PI3K/Akt/mTOR pathway in muscle and ameliorates pathology in a mouse model of Duchenne muscular dystrophy. *Am. J. Pathol.* **174,** 999–1008
27. Guerron, A. D., Rawat, R., Sali, A., Spurney, C. F., Pistilli, E., Cha, H. J., Pandey, G. S., Gernapudi, R., Francia, D., Farajian, V., Escolar, D. M., Bossi, L., Becker, M., Zerr, P., de la Porte, S., Gordish-Dressman, H., Partridge, T., Hoffman, E. P., and Nagaraju, K. (2010) Functional and molecular effects of arginine butyrate and prednisone on muscle and heart in the *mdx* mouse model of Duchenne muscular dystrophy. *PLoS One* **5,** e11220
28. Jeng, M. R., Feusner, J., Skibola, C., and Vichinsky, E. (2002) Central venous catheter complications in sickle cell disease. *Am. J. Hematol.* **69,** 103–108
29. Perrine, S. P., and Faller, D. V. (1993) Butyrate-induced reactivation of the fetal globin genes: a molecular treatment for the beta-hemoglobinopathies. *Experientia* **49,** 133–137
30. Baby, S. M., Bogdanovich, S., Willmann, G., Basu, U., Lozynska, O., and Khurana, T. S. (2010) Differential expression of utrophin-A and -B promoters in the central nervous system (CNS) of normal and dystrophic mdx mice. *Brain Pathol.* **20,** 323–342
31. Straub, V., Rafael, J. A., Chamberlain, J. S., and Campbell, K. P. (1997) Animal models for muscular dystrophy show different patterns of sarcolemmal disruption. *J. Cell Biol.* **139,** 375–385
32. Edom, F., Mouly, V., Barbet, J. P., Fiszman, M. Y., and Butler-Browne, G. S. (1994) Clones of human satellite cells can express in vitro both fast and slow myosin heavy chains. *Dev. Biol.* **164,** 219–229
33. Ozawa, E., Yoshida, M., Suzuki, A., Mizuno, Y., Hagiwara, Y., and Noguchi, S. (1995) Dystrophin-associated proteins in muscular dystrophy. *Hum. Mol. Genet.* **4,** 1711–1716
34. Nico, B., Paola Nicchia, G., Frigeri, A., Corsi, P., Mangieri, D., Ribatti, D., Svelto, M., and Roncali, L. (2004) Altered blood-brain barrier development in dystrophic MDX mice. *Neuroscience* **125,** 921–935
35. Colussi, C., Gurtner, A., Rosati, J., Illi, B., Ragone, G., Piaggio, G., Moggio, M., Lamperti, C., D'Angelo, G., Clementi, E., Minetti, G., Mozzetta, C., Antonini, A., Capogrossi, M. C., Puri, P. L., and Gaetano, C. (2009) Nitric oxide deficiency determines global chromatin changes in Duchenne muscular dystrophy. *FASEB J.* **23,** 2131–2141
36. Faller, D. V., and Perrine, S. P. (1995) Butyrate in the treatment of sickle cell disease and β-thalassemia. *Curr. Opin. Hematol.* **2,** 109–117
37. Perrine, S. P., Ginder, G. D., Faller, D. V., Dover, G. H., Ikuta, T., Witkowska, H. E., Cai, S. P., Vichinsky, E. P., and Olivieri, N. F. (1993) A short-term trial of butyrate to stimulate fetal-globin-gene expression in the beta-globin disorders. *N. Engl. J. Med.* **328,** 81–86
38. Perrine, S. P., Olivieri, N. F., Faller, D. V., Vichinsky, E. P., Dover, G. J., and Ginder, G. D. (1994) Butyrate derivatives. New agents for stimulating fetal globin production in the β-globin disorders. *Am. J. Pediatr. Hematol. Oncol.* **16,** 67–71
39. Sher, G. D., Ginder, G. D., Little, J., Yang, S., Dover, G. J., and Olivieri, N. F. (1995) Extended therapy with intravenous arginine butyrate in patients with β-hemoglobinopathies. *N. Engl. J. Med.* **332,** 1606–1610
40. Matsumura, K., and Campbell, K. P. (1994) Dystrophin-glycoprotein complex: its role in the molecular pathogenesis of muscular dystrophies. *Muscle Nerve* **17,** 2–15
41. Bia, B. L., Cassidy, P. J., Young, M. E., Rafael, J. A., Leighton, B., Davies, K. E., Radda, G. K., and Clarke, K. (1999) Decreased myocardial nNOS, increased iNOS and abnormal ECGs in mouse models of Duchenne muscular dystrophy. *J. Mol. Cell. Cardiol.* **31,** 1857–1862
42. Finsterer, J., and Stollberger, C. (2003) The heart in human dystrophinopathies. *Cardiology* **99,** 1–19
43. Ishikawa, K. (1997) Cardiac involvement in progressive muscular dystrophy of the Duchenne type. *Jpn. Heart J.* **38,** 163–180
44. Anderson, J. L., Head, S. I., Rae, C., and Morley, J. W. (2002) Brain function in Duchenne muscular dystrophy. *Brain* **125,** 4–13
45. Perronnet, C., Chagneau, C., Le Blanc, P., Samson-Desvignes, N., Mornet, D., Laroche, S., De La Porte, S., and Vaillend, C. (2012) Upregulation of brain utrophin does not rescue behavioral alterations in dystrophin-deficient mice. *Hum. Mol. Genet.* **21,** 2263–2276
46. Fisher, R., Tinsley, J. M., Phelps, S. R., Squire, S. E., Townsend, E. R., Martin, J. E., and Davies, K. E. (2001) Non-toxic ubiquitous over-expression of utrophin in the *mdx* mouse. *Neuromuscul. Disord.* **11,** 713–721
47. Salimena, M. C., Lagrota-Candido, J., and Quirico-Santos, T. (2004) Gender dimorphism influences extracellular matrix expression and regeneration of muscular tissue in *mdx* dystrophic mice. *Histochem. Cell Biol.* **122,** 435–444
48. Marbini, A., Gemignani, F., Bellanova, M. F., Guidetti, D., and Ferrari, A. (1996) Immunohistochemical localization of utrophin and other cytoskeletal proteins in skin smooth muscle in neuromuscular diseases. *J. Neurol. Sci.* **143,** 156–160
49. Tanveer, N., Sharma, M. C., Sarkar, C., Gulati, S., Kalra, V., Singh, S., and Bhatia, R. (2009) Diagnostic utility of skin biopsy in dystrophinopathies. *Clin. Neurol. Neurosurg.* **111,** 496–502
50. Anderson, J. E. (2000) A role for nitric oxide in muscle repair: nitric oxide-mediated activation of muscle satellite cells. *Mol. Biol. Cell* **11,** 1859–1874
51. Guilhermet, R. G. (1996) Fonctions nutritionnelles et métaboliques de l'arginine. *INRA Prod. Anim.* **9,** 265–272